Original Paper

Ophthalmologica

Ophthalmologica 2011;226:228–233
DOI: 10.1159/000331218

Received: May 3, 2011
Accepted after revision: July 19, 2011
Published online: September 1, 2011

Ultrastructure of the Membrana Limitans Interna after Dye-Assisted Membrane Peeling

Tobias Brockmann[a] Claudia Steger[a] Martin Westermann[b] Sandor Nietzsche[b]
Ekkehart Koenigsdoerffer[a] Juergen Strobel[a] Jens Dawczynski[c]

[a]Department of Ophthalmology and [b]Electron Microscopy Center, University Hospital Jena, Jena, and
[c]Department of Ophthalmology and Eye Hospital, Faculty of Medicine, University of Leipzig, Leipzig, Germany

Key Words
Macular hole surgery · Pars plana vitrectomy · Membrana limitans interna · Ultrastructure · Brilliant blue G · Indocyanine green · Membrane peeling

Abstract
The purpose of this study was to investigate the ultrastructure of the membrana limitans interna (internal limiting membrane, ILM) and to evaluate alterations to the retinal cell layers after membrane peeling with vital dyes. Twenty-five patients (25 eyes) who underwent macular hole surgery were included, whereby 12 indocyanine green (ICG)- and 13 brilliant blue G (BBG)-stained ILM were analyzed using light, transmission electron and scanning electron microscopy. Retinal cell fragments on the ILM were identified in both groups using immunohistochemistry. Comparing ICG- and BBG-stained membranes, larger cellular fragments were observed at a higher frequency in the BBG group. Thereby, the findings indicate that ICG permits an enhanced separation of the ILM from the underlying retina with less mechanical destruction. A possible explanation might be seen in the known photosensitivity of ICG, which induces a stiffening and shrinkage of the ILM but also generates retinal toxic metabolites.

Introduction

The internal limiting membrane (ILM) is the innermost layer of the retina and part of the vitreoretinal interface. Morphologically, the ILM is the basal membrane of the Müller glia, which plays an essential role in the homeostasis and stability of the retina [1]. In this context, retinal glial cells are responsible for the removal and metabolization of neurotransmitters such as γ-aminobutyric acid (GABA) [2]. The basal membrane consists of collagen fibers [3] and is tightly linked to the vitreous body by glycoproteins such as laminin and fibronectin [4, 5]. Thus, the ILM has to compensate for forces arising between the vitreous body and the retinal surface [6]. An imbalance in the affecting forces on the ILM, such as those caused by traction maculopathy, raises the risk of membrane destruction. In particular, the macular is predisposed to a disruption that can result in a macular hole [7]. The state of the art therapeutic intervention for macular holes is a pars-plana vitrectomy followed by an ILM peeling [8]. An additionally applied ILM staining with vital dyes prior to the peeling has been shown to improve the initial reattachment rate and the postoperative visual acuity [9]. Currently, indocyanine green (ICG) and brilliant blue G (BBG) are the most promising dyes for chro-

KARGER

Fax +41 61 306 12 34
E-Mail karger@karger.ch
www.karger.com

0030–3755/11/2264–0228$38.00/0

Accessible online at:
www.karger.com/oph

Jens Dawczynski
Department of Ophthalmology and Eye Hospital
Faculty of Medicine, University of Leipzig
Liebigstrasse 10–14, DE–04103 Leipzig (Germany)
Tel. +49 341 97 21650, E-Mail Jens.Dawczynski@medizin.uni-leipzig.de

Table 1. Clinical features of 25 eyes with a macular hole

Patient No./ Sex	Preparation technique	Age years	Dye	Eye	Lens status	Symptom duration, months	Best-corrected visual acuity	Macular hole stage
1/F	TEM/SEM	67	BBG	right	phakic/cat.	4	0.32	3
2/M	TEM/SEM	77	BBG	right	phakic/cat.	6	0.10	2
3/F	TEM/SEM	67	BBG	left	phakic/cat.	12	0.16	3
4/M	TEM/SEM	58	BBG	left	phakic/cat.	>12	0.16	4
5/M	TEM/SEM	56	BBG	left	phakic/cat.	6	0.10	4
6/F	TEM	79	BBG	left	phakic/cat.	NA	0.10	3
7/F	TEM	63	BBG	left	phakic/cat.	2	0.10	1b
8/F	SEM	65	BBG	left	phakic/cat.	6	0.10	4
9/F	SEM	68	BBG	left	phakic/cat.	5	0.32	3
10/F	TEM/SEM	71	BBG	right	phakic/cat.	6	0.40	3
11/F	TEM/SEM	82	BBG	right	pseudophakic	1	0.20	4
12/F	TEM	71	BBG	left	phakic/cat.	>12	0.32	1b
13/F	TEM	68	ICG	left	phakic/cat.	12	0.25	2
14/F	TEM/SEM	63	ICG	right	pseudophakic	6	0.20	1b
15/M	TEM/SEM	70	ICG	left	pseudophakic	12	0.08	4
16/F	TEM/SEM	74	ICG	left	phakic/cat.	2	0.32	2
17/F	TEM	66	ICG	right	phakic/cat.	NA	0.05	3
18/F	TEM/SEM	71	ICG	right	pseudophakic	4	0.32	4
19/F	TEM	74	ICG	right	phakic/cat.	3	0.10	3
20/F	TEM/SEM	73	ICG	right	pseudophakic	6	0.05	3
21/F	TEM	81	ICG	left	pseudophakic	NA	0.25	2
22/M	TEM	10	ICG	left	phakic	4	0.05	4
23/F	SEM	73	ICG	right	phakic/cat.	>12	0.32	3
24/F	SEM	73	ICG	left	phakic/cat.	3	0.20	2
25/M	SEM	75	ICG	right	pseudophakic	5	0.60	2

NA = No answer.

movitrectomy, even though there are controversial studies about the side effects. In particular, ICG is supposed to bring about a dose- and illumination-dependent toxicity [10, 11] to the retinal ganglion cells and the retinal pigment epithelium [12, 13]. However, regarding the functional outcome of ILM peeling with ICG or BBG after a period of 6 months, no significant differences were found [14]. Therefore, the intention of this study was to examine ultrastructural features on the ILM by ICG or BBG to gain a picture of retinal alterations secondary to membrane peeling.

Patients and Methods

Twenty-five eyes from 25 patients with a diagnosed macular hole according to Gass [15] were enrolled in this retrospective study. All individuals were undergoing their first surgery for macular hole repair. The study was undertaken between March 2008 and September 2009, in accordance with the rules of the local institutional review board and ethics committee. Benefits and risks of the pars-plana vitrectomy with vital dye-assisted membrane peeling were explained in detail to the patients, and the surgery was performed after written informed consent. The patient group consisted of 19 women and 6 men with a mean age of 68 years, ranging from 10 to 82 years. Fourteen left eyes and 11 right eyes were operated. The preoperative ophthalmic examination included Snellen visual acuity, intraocular pressure, slit-lamp examination, stereoscopic biomicroscopic examination and optical coherence tomography. For ILM staining, either 0.5 ml of 0.025% BBG (Brilliant Peel®, Fluoron GmbH; Neu-Ulm, Germany) or 0.3 ml of 0.1% ICG (ICG-Pulsion®, Pulsion AG; Munich, Germany) were used according to the schedule shown in table 1. BBG was applied to 12 patients, 9 women and 3 men, with a mean age of 69 years, ranging from 56 to 82 years. Membrane staining with ICG was performed in 13 patients, 10 women and 3 men, with an average age of 68 years, ranging from 10 to 81 years.

All eyes received a standard 23-gauge 3-port pars-plana vitrectomy with a posterior vitreous detachment. For surgical field illumination, a cold light source (Megatron®, Geuder AG, Heidelberg, Germany) was used. The vital dyes were applied over the macular and washed within 20 s. Subsequently, the stained ILM was gripped carefully and peeled in a maculorhexis fashion with Eckardt end-gripping ILM forceps (DORC BV, Zuidland, The Netherlands). The surgery was completed by a fluid-gas exchange

using hexafluoroethane (C_2F_6). Postoperatively, all patients were asked to remain in a facedown position for the following 7 days.

Intraoperatively, all harvested membranes were placed into 4% formaldehyde and stored at 4°C overnight for fixation. During the removal procedure, the ILM folded up into a small multilayered fragment. For this reason and handling circumstances, fragments smaller than 4 mm^2 were used for light and transmission electron microscopy (TEM), whereas larger fragments were used for scanning electron microscopy (SEM). The group characteristics according to the preparation technique are summarized in table 2.

Concerning SEM, the membranes were fixed for 2 h in 2% glutaraldehyde in 0.1 M sodium-cacodylate buffer. Afterwards, the specimens were dehydrated for 2 h in an ascending ethanol series. A terminal structure preservation was accomplished by critical point drying with carbon dioxide (CPD 30, BAL-TEC AG, Balzers, Liechtenstein), followed by gold sputtering (SCD 005, BAL-TEC AG). Finally, the membranes were examined on a LEO 1450 VP scanning electron microscope (Carl Zeiss AG, Oberkochen, Germany).

Membrane fragments intended for TEM were first prepared for gold spotted immunohistochemistry using $GABA_A$ receptor α1 antibodies (Santa Cruz Biotechnology Inc., Santa Cruz, Calif., USA). Afterwards, the specimens were fixed for 4 h in 4% glutaraldehyde in 0.1 M sodium-cacodylate buffer, followed by postfixation (2 h) in 1% OsO_4 in sodium-cacodylate buffer. The membranes were dehydrated within alcohol and contrasted in 1% uranyl acetate. A terminal dehydration was accomplished in propylene oxide. The specimens were infiltrated with araldite resin and curing was performed for 48 h at 60°C. Particular attention was paid to cut all embedded membranes perpendicularly into semi-thin (2 μm) and ultrathin (70 nm) slices by a diamond knife using a LKB 8800A Ultratome III (LKB Produkter AB, Bromma, Sweden). Finally, semi-thin slices were stained with Richardson's blue [16] for light microscopic examination (Axioskop 2 MOT, Carl Zeiss AG; Jena, Germany). Accordingly, ultrathin slices were contrasted with lead citrate for viewing in an EM 902A transmission electron microscope (Carl Zeiss AG; Oberkochen, Germany).

A skilled and blinded observer accomplished the examination of all electron microscopic images using ImageJ software v. 1.41 (National Institutes of Health; Bethesda, Md., USA). The statistical analyses were accomplished using SPSS software v. 17.0 (SPSS Inc., Chicago, Ill., USA). A p value less than 0.05 was considered to be statistically significant.

Table 2. Baseline characteristics of the study groups

	TEM		SEM	
	BBG (n = 10)	ICG (n = 10)	BBG (n = 9)	ICG (n = 8)
Age, years				
Minimum	56	10	56	63
Maximum	82	81	82	75
Mean	69.1	65.0	67.9	71.5
SD	8.7	20.0	8.2	3.8
Sex				
Female	7 (70)	8 (80)	6 (67)	6 (75)
Eye				
Left eye	6 (60)	5 (50)	5 (56)	3 (38)
Preop. visual acuity				
Minimum	0.10	0.05	0.10	0.05
Maximum	0.40	0.30	0.40	0.60
Mean	0.19	0.16	0.20	0.25
SD	0.11	0.11	0.11	0.17

Figures in parentheses are percentages.

Results

An ILM was observed in all biopsies prepared for electron microscopy. Twenty specimens, 10 BBG- and 10 ICG-stained ILM, were prepared for light microscopy and TEM examinations. Light microscopy (not shown) was solely used to assure an adequate preparation quality of the biopsies. TEM was used for a detailed examination of the ILM, the determination of the membrane thickness and the analysis of residual cell fragments as shown in figure 1. The average ILM thickness was 2.00 ± 0.39 μm (median 1.97 μm) after ICG staining and 2.48 ± 0.31 μm (median 2.48 μm) after BBG application. Comparing the thicknesses, we found a Gaussian distribution with a significant difference between the two groups (p = 0.007, Student's t test). On the retinal side of the ILM, ruptured cell fragments were investigated. On the one hand, lipid bilayers were identified at a magnification of ×20,000 and, on the other hand, immunogold labeling with $GABA_A$ receptor α1 antibodies was performed. The detection was positive in 9 of 10 cases (90%) within the ICG group and 8 of 9 cases (89%) within the BBG group. One ICG-stained ILM served as a negative control. With regard to the quantification of those cell fragments, we identified 13.8 ± 3.8 fragments per 10 μm membrane length (median 12.8 fragments per 10 μm) in ICG-stained ILM and 19.2 ± 6.1 fragments per 10 μm membrane length (median 18.2 fragments per 10 μm) in BBG-stained membranes. Comparing the two groups, we found a significant difference (p = 0.028, Wilcoxon-Mann-Whitney test). As shown in figure 2, the surface of 9 BBG- and 8 ICG-stained membranes was examined using SEM. The smooth vitreal surface was easily distinguishable from the rough retinal surface with numerous vesicular structures. The average diameter of the present vesicular structures was 0.16 ± 0.06 μm (median 0.14 μm) after ICG staining and 0.22 ± 0.04 μm (median 0.24 μm) after BBG application. Comparing the diameters, we

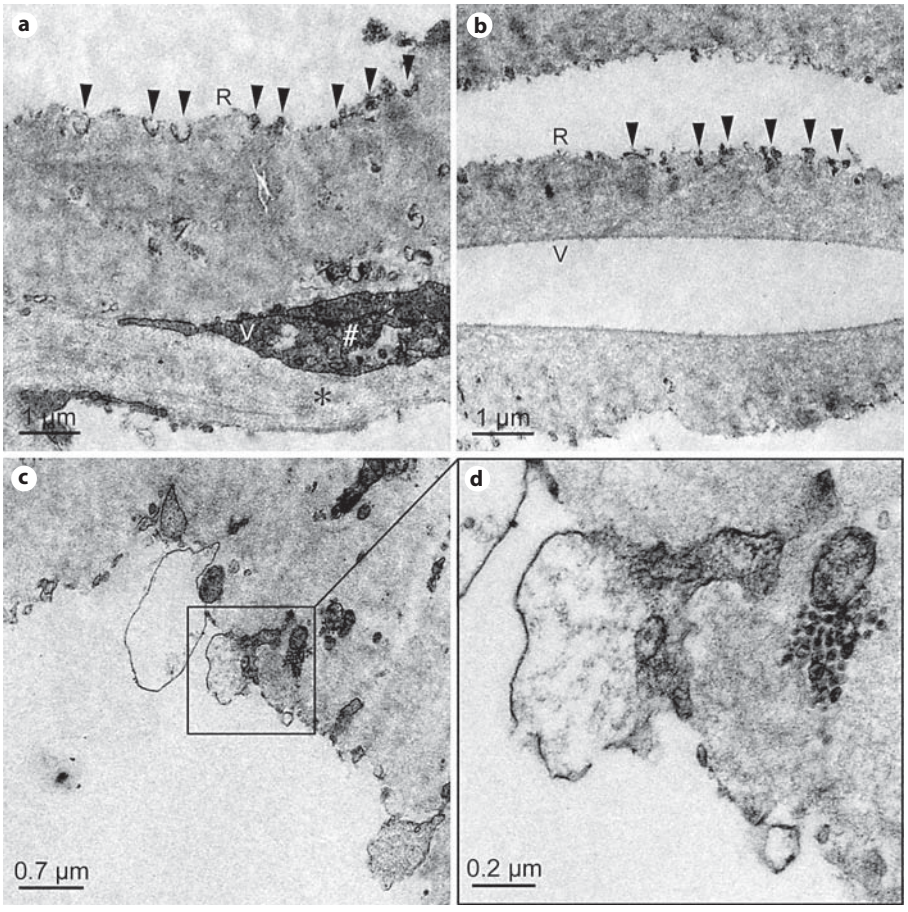

Fig. 1. Transmission electron microscopic images of the ILM. The retinal (R) and the vitreal (V) sides of BBG- (**a**, **c** and **d**) and ICG- (**b**) stained ILM were highly distinguishable. On the vitreal membrane side, collagen matrix (asterisk in **a**) and vitreous cells (hash in **a**) were observed occasionally. On the retinal ILM side, cellular fragments (arrowheads in **a** and **b**) were found in all specimens. Single cell fragments are presented as vesicular structures in **c** and under higher magnification in **d**.

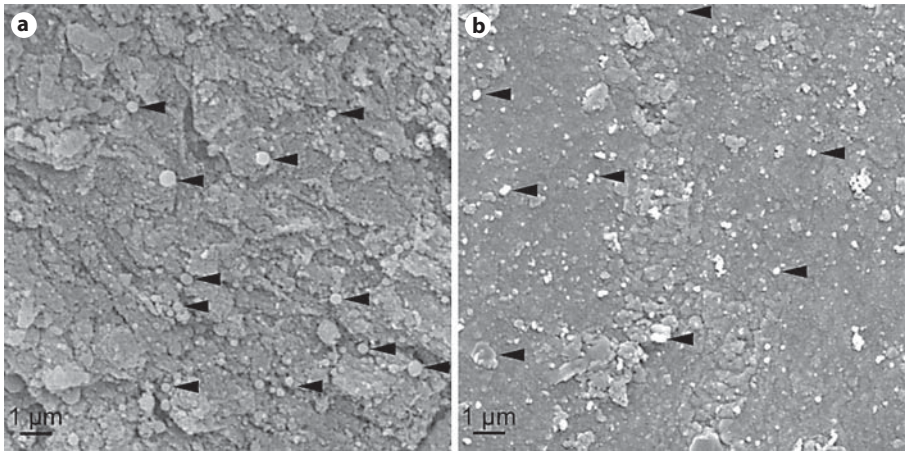

Fig. 2. The retinal surface of the ILM in scanning electron microscopy. Cellular fragments were observed as spheroid structures (arrowheads) on the rough surface of the collagen matrix on BBG- (**a**) and ICG- (**b**) stained membranes. They were identified as inner portions of Müller glia.

found a significant difference between the two groups ($p = 0.021$, Wilcoxon-Mann-Whitney test).

Concerning the postoperative anatomical outcome, we observed a macular hole closure in 24 of 25 eyes (96%). A persistent foveal defect was observed in one long-standing stage 4 hole (patient No. 15). The functional outcome was examined in a short-term follow-up after 1 month. On average, patients with ICG peeling gained 9.4 letters compared to 6.8 letters with BBG peeling; no significant difference was found ($p = 0.762$, Student's t test).

Conclusions

Selective ILM peeling around the macular hole has been proven to be a necessary requirement for the successful anatomic and functional reorganization of foveal defects [17]. An additional ILM staining turned out to be favorable by contrasting the translucent membrane to grip the ILM and to differentiate peeled from non-peeled areas on the macular [18]. In this context, ICG and BBG displayed sufficient and selective staining characteristics [19]. The first dye used for ILM peeling was ICG, and this has been extensively investigated. In the last years, ICG has been discredited because of its phototoxic properties [20]. Uemura et al. [21] observed visual field defects after membrane peeling with ICG. Further long-term follow-up investigations have shown that these functional defects continue to deteriorate over the following years and the nerve fiber layer degrades [22, 23]. Following this, BBG was established as a promising alternative biocompatible staining substance [24, 25]. However, later in vitro investigations also demonstrated a retinal toxicity of BBG [26, 27].

In our study, we analyzed the influence of ICG and BBG on vitreoretinal integrity when used as vital dyes for membrane peeling during macular hole surgery. $GABA_A$ receptor α1 antibodies were used to identify cellular fragments of Müller glia on the ILM, which were found in both study groups. It is known that GABA receptors are unevenly distributed across the Müller cell membrane, with a higher density at the endfoot that merges into the ILM [28]. A quantification of the adjacent cell fragments has shown a significantly higher amount of residues on BBG-stained ILM. In a parallel approach, the retinal ILM surface was analyzed using SEM. For the first time, Jerry Sebag [29] identified vesicles on the retinal ILM surface by SEM as inner portions of Müller glia. The measurement and analyses of those retinal vesicles has shown larger portions of Müller glia on BBG-stained ILM. The concurrent observation of more frequent and larger cellular fragments on the ILM might indicate that BBG-assisted membrane peeling induces a more profound alteration to the adjacent retinal cell layers than a peeling with ICG. A possible explanation of these findings could be seen in the photodynamic effect of ICG. So far, the photodegradable properties have primarily been discussed in regard to the cytotoxicity [30]. However, our observations indicate that biomechanical alterations of the ILM after ICG staining strongly influence the definite separation of the membrane while peeling [31]. In this context, we also observed a significantly reduced thickness within ICG-stained ILM, compared to BBG-stained specimens. Similar to corneal cross-linking with riboflavin and UVA light [32], ICG apparently leads to an increase in the biomechanical stability and a shrinkage of the ILM. This might explain the subjective sensation of some surgeons that ICG-assisted maculorhexis is more comfortable to perform and a rupture of the membrane is unlikely.

Unfortunately, the preferable biomechanical properties of ICG are inextricably linked to its photolysis that generates cytotoxic metabolites [33]. Future generations of staining substances should ideally cover both aspects to dispel current skepticism of dye-assisted macular surgery.

Regarding the functional results, this ultrastructural study is limited due to the brief follow-up period. Correspondingly, we did not find a difference in the functional outcome between the two groups. Large long-term interventional case studies have shown that the entire rearrangement of the macula requires several months [34]. For this reason, further investigations are needed.

References

1 Lundkvist A, Reichenbach A, Betsholtz C, Carmeliet P, Wolburg H, Pekny M: Under stress, the absence of intermediate filaments from Muller cells in the retina has structural and functional consequences. J Cell Sci 2004; 117:3481–3488.

2 Bringmann A, Pannicke T, Biedermann B, Francke M, Iandiev I, Grosche J, Wiedemann P, Albrecht J, Reichenbach A: Role of retinal glial cells in neurotransmitter uptake and metabolism. Neurochem Int 2009;54:143–160.

3 Ponsioen TL, van Luyn MJ, van der Worp RJ, van Meurs JC, Hooymans JM, Los LI: Collagen distribution in the human vitreoretinal interface. Invest Ophthalmol Vis Sci 2008;49:4089–4095.

4 Kohno T, Sorgente N, Ishibashi T, Goodnight R, Ryan S: Immunofluorescent studies of fibronectin and laminin in the human eye. Invest Ophthalmol Vis Sci 1987;28:506–514.

5 Russell S, Shepherd J, Hageman G: Distribution of glycoconjugates in the human retinal internal limiting membrane. Invest Ophthalmol Vis Sci 1991;32:1986–1995.

6 Matsumoto B, Blanks J, Ryan S: Topographic variations in the rabbit and primate internal limiting membrane. Invest Ophthalmol Vis Sci 1984;25:71–82.

7 Bainbridge J, Herbert E, Gregor Z: Macular holes: vitreoretinal relationships and surgical approaches. Eye 2008;22:1301–1309.

8 Korda V, Dusova D, Studnicka J, Rencova E, Hejcmanova D: The surgical management of macular hole (in Czech). Cesk Slov Oftalmol 2005;61:316–320.

9 Oie Y, Emi K, Takaoka G, Ikeda T: Effect of indocyanine green staining in peeling of internal limiting membrane for retinal detachment resulting from macular hole in myopic eyes. Ophthalmology 2007;114:303–306.
10 Gandorfer A, Haritoglou C, Kampik A: Toxicity of indocyanine green in vitreoretinal surgery. Dev Ophthalmol 2008;42:69–81.
11 Enaida H, Sakamoto T, Hisatomi T, Goto Y, Ishibashi T: Morphological and functional damage of the retina caused by intravitreous indocyanine green in rat eyes. Graefes Arch Clin Exp Ophthalmol 2002;240:209–213.
12 Rodrigues E, Meyer C, Mennel S, Farah M: Mechanisms of intravitreal toxicity of indocyanine green dye: Implications for chromovitrectomy. Retina 2007;27:958–970.
13 Iriyama A, Uchida S, Yanagi Y, Tamaki Y, Inoue Y, Matsuura K, Kadonosono K, Araie M: Effects of indocyanine green on retinal ganglion cells. Invest Ophthalmol Vis Sci 2004;45:943–947.
14 Schmid-Kubista K, Lamar P, Schenk A, Stolba U, Binder S: Comparison of macular function and visual fields after membrane blue or infracyanine green staining in vitreoretinal surgery. Graefes Arch Clin Exp Ophthalmol 2010;248:381–388.
15 Gass J: Idiopathic senile macular hole: its early stages and pathogenesis. Arch Ophthalmol 1988;106:629–639.
16 Richardson K, Jarett L, Finke E: Embedding in epoxy resins for ultrathin sectioning in electron microscopy. Stain Technol 1960;35:313–323.
17 Lois N, Burr JM, Norrie J, Vale L, Cook JA, McDonald A, Boachie C, Ternent L, McPherson G: Internal limiting membrane peeling versus no peeling for idiopathic full thickness macular hole: a pragmatic randomised controlled trial. Invest Ophthalmol Vis Sci 2011;52:1586–1592.
18 Kwok AK, Lai TY, Man-Chan W, Woo DC: Indocyanine green assisted retinal internal limiting membrane removal in stage 3 or 4 macular hole surgery. Br J Ophthalmol 2003;87:71–74.
19 Remy M, Thaler S, Schumann R, May C, Fiedorowicz M, Schuettauf F, Grüterich M, Priglinger S, Nentwich M, Kampik A, Haritoglou C: An in vivo evaluation of brilliant blue G in animals and humans. Br J Ophthalmol 2008;92:1142–1147.
20 Engel E, Schraml R, Maisch T, Kobuch K, Konig B, Szeimies RM, Hillenkamp J, Baumler W, Vasold R: Light-induced decomposition of indocyanine green. Invest Ophthalmol Vis Sci 2008;49:1777–1783.
21 Uemura A, Kanda S, Sakamoto Y, Kita H: Visual field defects after uneventful vitrectomy for epiretinal membrane with indocyanine green-assisted internal limiting membrane peeling. Am J Ophthalmol 2003;136:252–257.
22 Yamashita T, Uemura A, Kita H, Nakao K, Sakamoto T: Long-term outcomes of visual field defects after indocyanine green-assisted macular hole surgery. Retina 2008;28:1228–1233.
23 Yamashita T, Uemura A, Kita H, Sakamoto T: Analysis of the retinal nerve fiber layer after indocyanine green-assisted vitrectomy for idiopathic macular holes. Ophthalmology 2006;113:280–284.
24 Ueno A, Hisatomi T, Enaida H, Kagimoto T, Mochizuki Y, Goto Y, Kubota T, Hata Y, Ishibashi T: Biocompatibility of brilliant blue G in a rat model of subretinal injection. Retina 2007;27:499–504.
25 Enaida H, Ishibashi T: Brilliant blue in vitreoretinal surgery. Dev Ophthalmol 2008;42:115–125.
26 Yuen D, Gonder J, Proulx A, Liu H, Hutnik C: Comparison of the in vitro safety of intraocular dyes using two retinal cell lines: a focus on brilliant blue G and indocyanine green. Am J Ophthalmol 2009;147:251–259.e252.
27 Morales M, Freire V, Asumendi A, Araiz J, Herrera I, Castiella G, Corcóstegui I, Corcóstegui G: Comparative effects of six intraocular vital dyes on retinal pigment epithelial cells. Invest Ophthalmol Vis Sci 2010;51:6018–6029.
28 Biedermann B, Bringmann A, Franze K, Faude F, Wiedemann P, Reichenbach A: Gaba(a) receptors in Muller glial cells of the human retina. Glia 2004;46:302–310.
29 Sebag J: Age-related differences in the human vitreoretinal interface. Arch Ophthalmol 1991;109:966–971.
30 Gandorfer A, Haritoglou C, Kampik A: Toxicity of indocyanine green in vitreoretinal surgery. Dev Ophthalmol 2008;42:69–81.
31 Wollensak G: Biomechanical changes of the internal limiting membrane after indocyanine green staining. Dev Ophthalmol 2008;42:82–90.
32 Wollensak G, Wilsch M, Spoerl E, Seiler T: Collagen fiber diameter in the rabbit cornea after collagen crosslinking by riboflavin/UVA. Cornea 2004;23:503–507.
33 Tokuda K, Zorumski C, Izumi Y: Involvement of illumination in indocyanine green toxicity after its washout in the ex vivo rat retina. Retina 2009;29:371–379.
34 Da Mata AP, Burk SE, Foster RE, Riemann CD, Petersen MR, Nehemy MB, Augsburger JJ: Long-term follow-up of indocyanine green-assisted peeling of the retinal internal limiting membrane during vitrectomy surgery for idiopathic macular hole repair. Ophthalmology 2004;111:2246–2253.